Jurnal Polimesin
Department of Mechanical Engineering
State Polytechnic of Lhokseumawe
http://e-jurnal.pnl.ac.id/polimesin
e-ISSN : 2549-1999 No. : 4 Month : August
p-ISSN : 1693-5462 Volume : 22 Year : 2024

Article Processing Dates: Received on 2024-03-11, Reviewed on 2024-05-01, Revised on 2024-07-30, Accepted on 2024-08-02 and Available online on 2024-08-30

Numerical study of downwash flow on rice plant protection drone using computational fluid dynamics method

Mohamad Yamin* **and Muhammad Zidan Alfasha**
Mechanical Engineering Department, Gunadarma University, Depok, 16424, Indonesia
*Corresponding author: mohay@staff.gunadarma.ac.id

Abstract

Unnamed Unmanned Aerial Vehicles (UAVs) are increasingly being utilized in various industries, including agriculture, to support the growing demand for food. UAVs streamline work processes and are particularly useful in the spraying method for plant protection. This study aims to analyze the characteristics of the downwash flow, which are influenced by factors such as flight altitude, airfoil profile, and the flying speed of the drone. Unlike previous studies that used 6-blade UAVs, this research focused on a 4-blade configuration. The study employed Computational Fluid Dynamics (CFD) to analyze drone geometry and input boundary conditions based on environmental factors. The drone's flying altitude significantly impacted downwash flow, particularly concerning In Ground Effect (IGE) and Out of Ground Effect (OGE) conditions. Unlike previous research, this study considered the airfoil profile of the propeller, which, along with the drag and lift coefficients from the airfoil geometry, affected the downwash flow. The drone's flying speed, related to the relative wind speed around its working area, also influenced pressure distribution and downwash flow speed. These factors significantly impacted downwash flow and determined the distribution of plant protection droplets on the rice field. The results indicated that increasing flight altitude reduced the ground effect, affecting the quadcopter's downwash. Similarly, flight speed had a similar effect on downwash as altitude. Based on these findings, the study recommended a flight altitude of 2 m and a speed of 2 m/s for optimal downwash and proper distribution of plant protection.

Keywords:
Plant protection, spray, CFD, drone, downwash, UAV.

1 Introduction

Modern UAV technology has been in use for over two decades, but its origins can be traced back to 1916. The inaugural UAV was named the "Hewitt-Sperry Automatic Plane," and its initial objective was to transport military flying bombs [1]. Recently, there has been a significant increase in the number of UAV studies [2].

Unmanned Aerial Vehicles (UAVs), generally speaking, can be classified based on two main aspects: design (classification by design) [3] and performance characteristics (classification by performance characteristic) [1]. In this particular study, a multirotor UAV with a quadcopter configuration was employed for use in the agricultural sector as a sprayer for plant protection purposes [4].

Agriculture plays a vital role in sustaining the global population's food requirements. UAVs have proven to be a more efficient, effective, and economical means of analyzing vegetative conditions [5]. With several years of development, agricultural drones have become widely utilized in modern agriculture [6]. UAVs have experienced rapid growth due to their ability to efficiently apply protective measures to densely planted crops [7]. Therefore, this field warrants attention for treatment, particularly in terms of spraying plant protection using pesticides [5].

Recent research has focused on the distribution and properties of downwash streams generated by UAVs used in crop protection. One prominent method involves employing an array of wind speed sensors to collect data for inversion modeling. Additionally, several journals have explored the optimal flight altitude for 6-rotor UAVs, taking into account downwash and ground effect considerations [8].

Downwash refers to changes in air direction caused by the aerodynamic forces of wings [9] or moving propellers that generate lift [1]. Furthermore, operational factors such as flight altitude, speed, and UAV type can impact downwash [10]. Downwash is closely linked to the ground effect phenomenon. When a UAV flies close to the ground, turbulence and pressure caused by the ground effect can disrupt the flow rate of droplets during plant protection spraying. Consequently, downwash can affect the distribution and penetration of droplets due to the positive relationship between wind speed and droplets [11].

Based on extensive research conducted on UAVs equipped with six rotors, it has been determined that the optimal flying height for UAVs engaged in plant protection spraying is 3 meters. This height, often referred to as the optimal height of the quadcopter UAV in spraying, takes into consideration the downwash flow [8]. The findings are based on Computational Fluid Dynamics (CFD) utilizing the transient method.

The flying height of the UAV has a significant impact on the spread of plant protection over paddy fields. Additionally, the flying speed of the quadcopter also affects the distribution of droplet protection on the land. The speed at which the drone flies influences the direction of the downwash, which, in turn, governs the flow of droplets carrying the plant protection solution. Consequently, the outcome of this study is the determination of the distance to which the plant protection solution is spread on the land. This is described by examining the pressure and velocity distribution at specific points on the land.

In contrast to previous studies that solely focused on flight speed and altitude, this latest research introduces an additional variable: blade geometry. The impact of the blade geometry on the downwash flow of the drone will be taken into account in this study.

The quadcopter design in this study, the body and frame become one unified part, where the assembly is on the body, which is the seat of the electric motor that will drive the propeller. This concept is expected to minimize assembly, facilitate maintenance, and provide more space in the body to place other electrical components (Fig. 1).

The body and frame specifications used in this study as shown in Table 1.

Table 1. Design specification

Quadcopter design		
Type	Diagonal wheelbase (cm)	Dimension (cm)
Stretch X	56	52 × 52 × 30

The propeller types used are NACA 0015 and NACA 4415, with a length of 12 inches (Fig. 2). The 3D design was made by using Solidworks 2020 software. The design is the geometry that will be simulated in the CFD software. The dimensions of each component are adjusted to the design calculations that have been calculated. By assembling the entire body frame and drone air propulsion system, the drone's overall dimensions and the design's center of gravity are obtained.

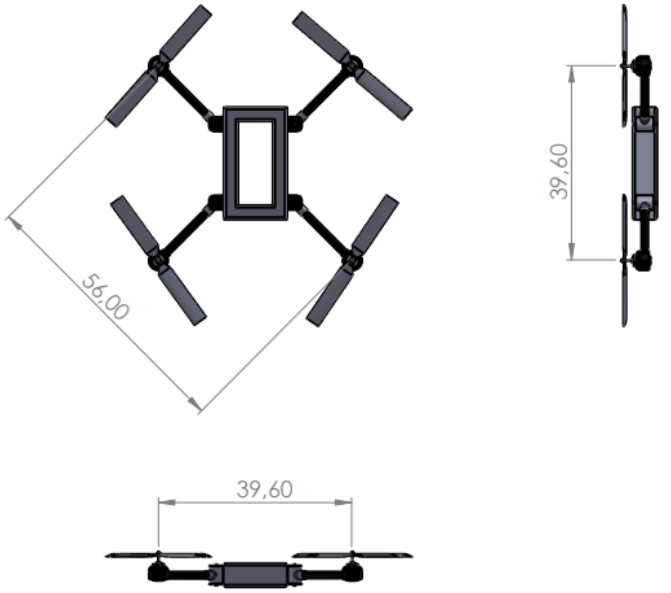

Fig. 1. Frame design of quadcopter.

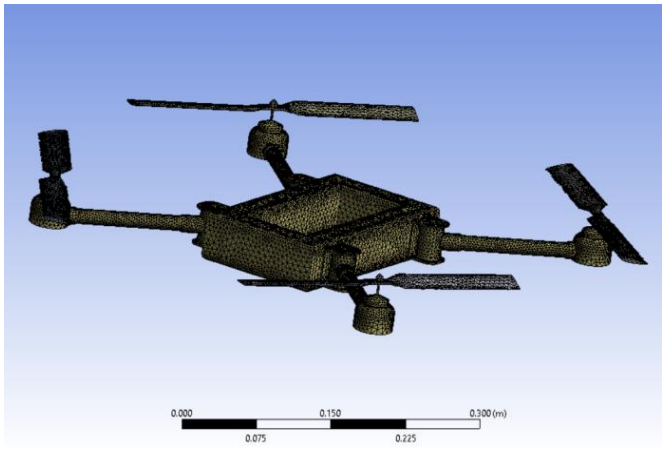

(a)

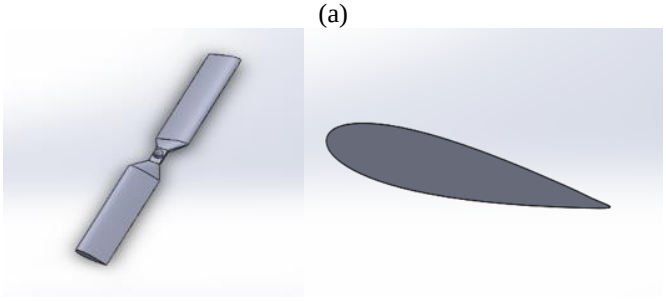

(b)

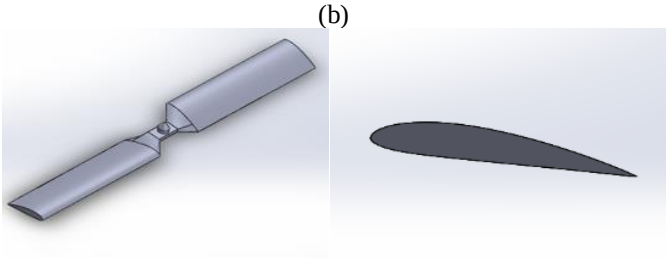

(c)

Fig. 2. Propeller and profile design (a) airfoil set up on geometry (b) NACA 0015 (c) NACA 4415.

2 Research Methods

This study aims to determine the downwash flow resulting from the propeller's operation on the quadcopter used for spraying plant protection. It also aims to forecast the distribution area of the plant protection on the land. The quadcopter serves as a tool to support modern agriculture in the spraying of plant protection. Based on existing literature, quadcopters have an advantage in terms of stability [12]. Additionally, the quadcopter's four rotors, with opposite rotations, compensate for the reacting pairs, providing the necessary power for vertical thrust. From this perspective, a quadcopter is more efficient than a conventional helicopter [13].

The selection of components related to the quadcopter air propulsion system in this study is based on the quadcopter design. This process provides mathematical information for determining the appropriate component specifications. The goal is to achieve suitable pairing between each component [14], resulting in a quadcopter that meets the required specifications. These specifications will then be implemented through the creation of 3D CAD drawings using Solidworks 2020 software.

During the application of spraying for crop protection, the downwash flow field of the UAV plays a crucial role in driving the spray drops onto the crops. The spray coverage and distribution directly impact the spray range, as well as droplet deposition and drift. Therefore, the operational effectiveness of the UAV can be significantly affected. This issue forms the central focus of the research discussion.

The propeller size is adjusted to match the motor and frame specifications of this quadcopter. A study was conducted to evaluate the quadcopter's flying altitude at 1 m, 2 m, 2.5 m, and 3 m heights. The quadcopter maintains a consistent speed of 1500 rpm at each altitude, utilizing the NACA 0015 propeller profile. Further research aims to determine the distribution area of plant protection, taking into account the drone's flight speed (1-5 m/s). Additionally, a comparison will be made between the NACA 0015 and NACA 4415 airfoil profiles in relation to the land, as described by the distribution of pressure and velocity of the downwash flow in rice fields.

Analysis of downwash flow due to propeller work on a quadcopter spraying plant protection has been investigated [15]. The downwash airflow will be known for its pressure and speed [16] through ANSYS R1 fluent software simulation. It started from the 3d design input, which becomes the software's geometry and creates a quadcopter work area (Fig. 3).

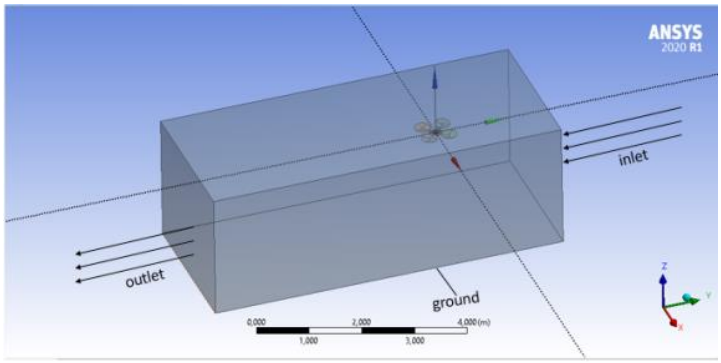

Fig. 3. Geometry domain.

Next, the meshing process is carried out by varying the number of elements from 50,000 to 6,000,000. This is done to determine the minimum number of meshes required to reduce computational costs. The meshing process is performed using the meshing feature in ANSYS, as shown in Fig. 4.

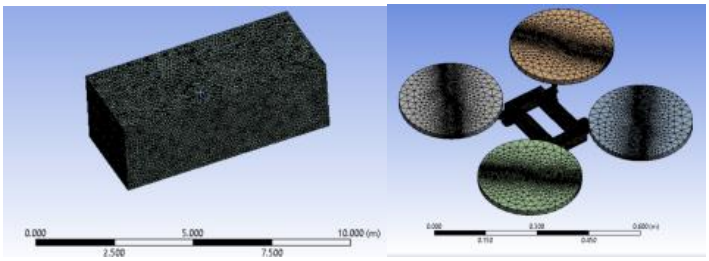

Fig. 4. Mesh used in simulation.

The results of the simulation for determining the values of CD and CL with varying mesh element quantities are shown in Fig. 5 and Fig. 6.

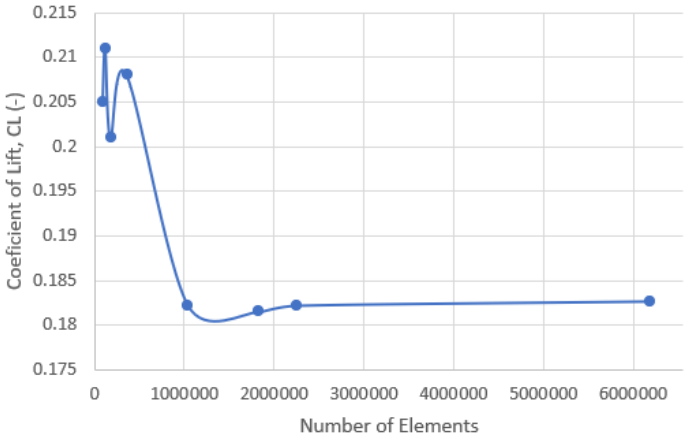

Fig. 5. Comparation No. of element vs CL.

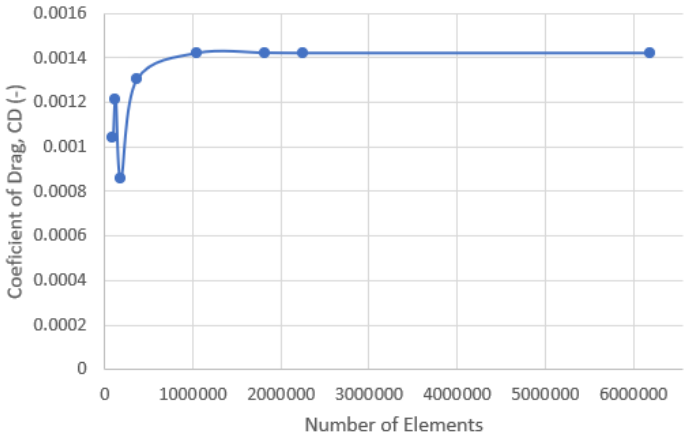

Fig. 6. Comparation No. of element vs CD.

Fig. 5 and Fig. 6 show the result of mesh independence will be stable with more than 2 milion up of number of element.

Based on the results of the mesh independence study, the simulation will be carried out using the boundary conditions listed in Table 2.

Table 2. Boundary condition

Model	Quadcopter scretch X	NACA 0014 and NACA 4415
Time scheme	Transient	
Viscous	k-w	
Mesh	Node : 722437	
	Element : 2872399	
Parameter	Inlet	2.2 m/s
	Outlet	Standard stationary outlet
	Wall	Standard Stationary wall
	Flight Speed	1 m/s
		2 m/s
		3 m/s
		4 m/s
		5 m/s
	Flight Height	1m
		2m
		2.5m
		3m

3 Results and Discussion

3.1 Quadcopter Flying Height

The results of the numerical analysis of the downwash flow on the quadcopter are shown in Fig. 7 for various flight altitudes of 1, 2, 2.5, and 3 m relative altitudes, respectively.

In this study, the speed of the motor is uniform for a certain height. The speed of each motor is 1500 rpm. The speed distribution for the UAV quadcopter is complexly illustrated in the Fig. 7.

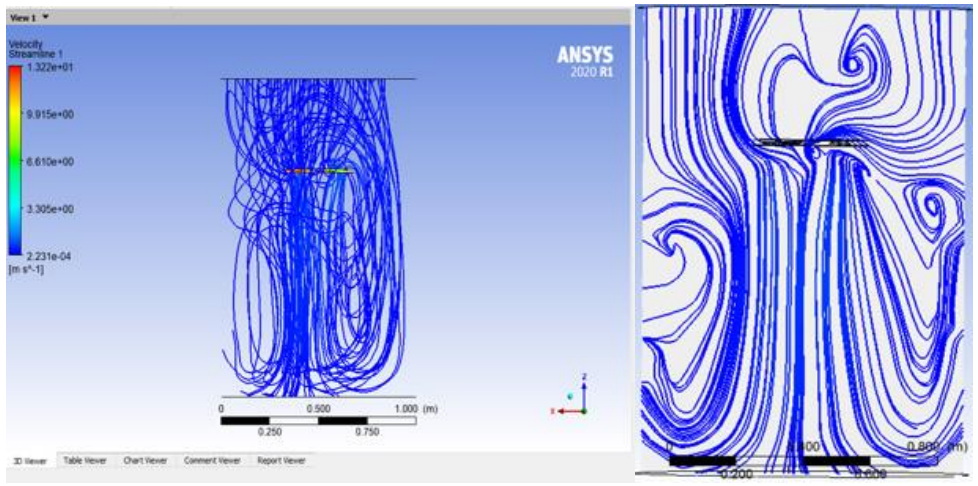

(a)

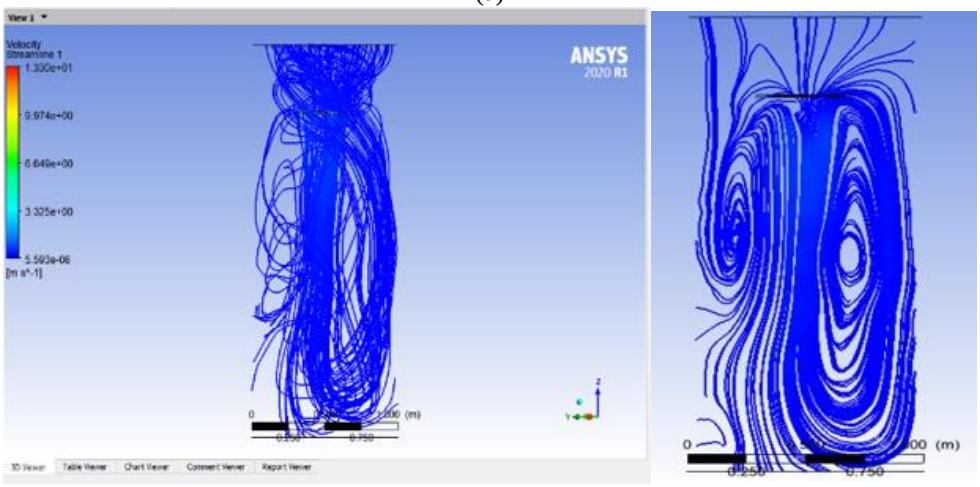

(b)

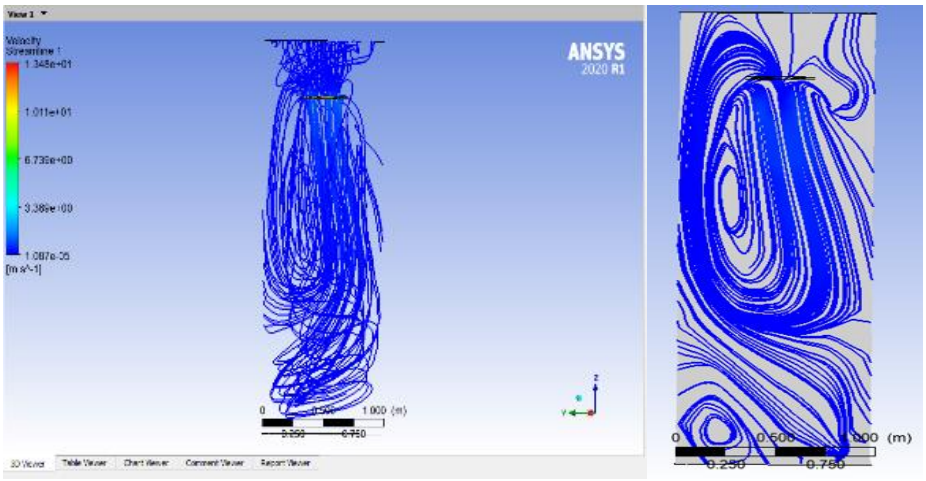

(c)

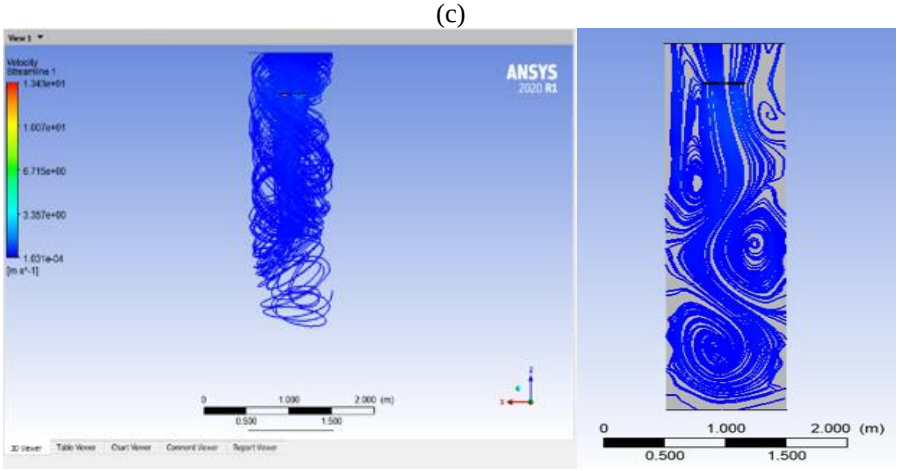

(d)

Fig. 7. Downwash flow velocity distribution (a) 1 m high, (b) 2 m high, (c) 2.5 m high, (d) 3 m high.

With increasing height, the trend of minimum flow velocity decreased from 1 m to 2 m height until it was close to zero, then increased again at 2.5 m and 3 m height. The density of the current lines is reflected by the ground effect. With increasing drift height, the ground effect decreases (Fig. 7). Therefore, compared to previous studies [17][18], the simulation results show the same outcome in terms of increasing the hover altitude. The ground effect (in ground effect) decreases, and the velocity flow becomes more concentrated until it decreases to 0. However, at the height when the quadcopter is in a certain area (of ground effect), the downwash flow no longer depends solely on soil effects but also on the speed of the surrounding air. This leads to instability and an increase in downwash flow velocity due to the surrounding air.

Regardless of hover height, airflow enters the rotor region from above and exits downwards (Fig. 7) in images taken in a vertical plane at the center of the body. However, as the drift height increases, the ground effect decreases and the flow field becomes more evenly distributed, causing the center to be more concentrated and move vertically downward. The downwash of the drone is directed due to the absence of the ground effect. Moreover, the turbulence in the fluid field is more stable, but the proportion of space occupied by the turbulence decreases compared to the entire UAV downwash flow plane. But at a certain height, the downwash flow no longer depends on the ground effect but also on the speed of the surrounding air, resulting in instability and reverse flow of the downwash flow due to the surrounding air.

The pressure distribution around the multi-rotor UAV at different heights, at 1, 2, 2.5, and 3m, is shown in Fig. 8.

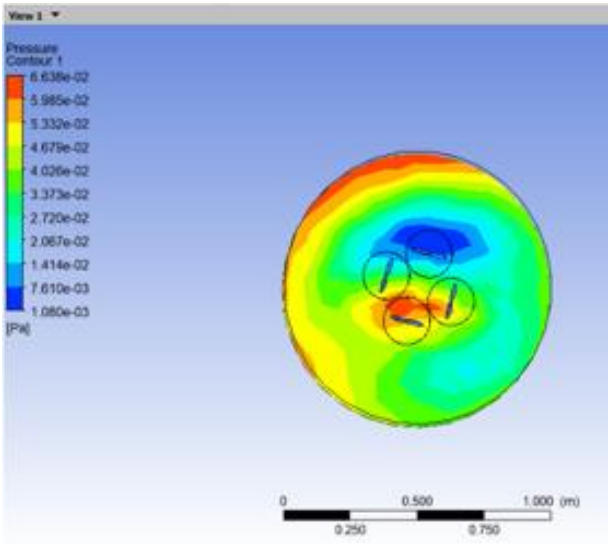

(a)

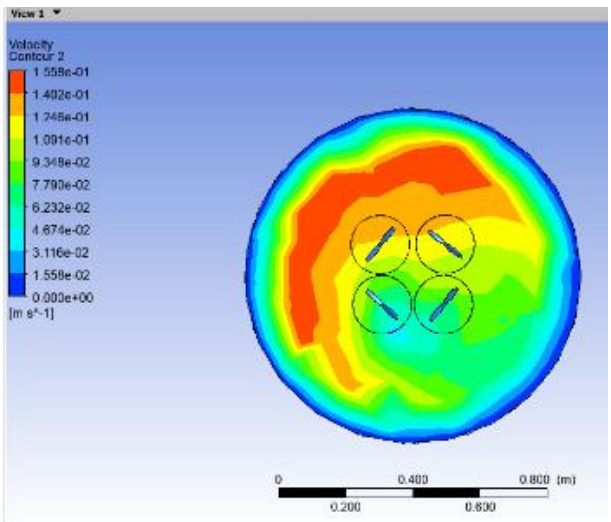

(b)

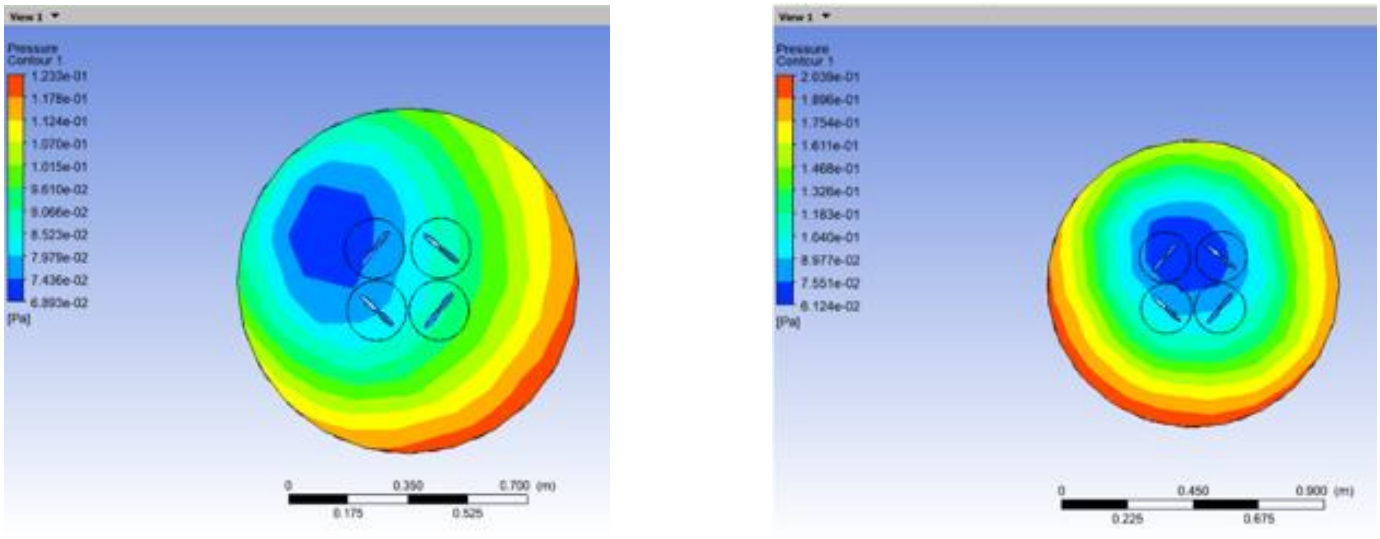

(c) (d)

Fig. 8. Downwash flow pressure distribution (a) 1 m high, (b) 2 m high, (c) 2.5 m high, (d) 3 m high.

The increased flight altitude results in a more uniform and symmetrical downwash flow field. Therefore, flight control of multi-rotor UAVs is challenging to predict manually and automatically.

These findings can still be considered consistent with previous research. Moreover, pesticides can be applied more uniformly, potentially leading to improved crop protection outcomes, which align with previous research findings. Reduced resistance to spray droplets may impact the penetration of the droplets. Furthermore, droplet deposition decreases, while droplet uniformity and penetration decrease as the spray width increases [19].

For practical spraying, it is crucial to select UAV operating parameters that ensure uniformity and droplet penetration. Meanwhile, the turbulence caused by the soil and surrounding air will have a significant effect, allowing the droplets to be deposited on the undersides of the leaves. Additionally, the spray width must be set at an appropriate value. Otherwise, a small spray width will prolong the duration of spraying. Taking into account these factors and the outcomes of a simulation involving a plant protection spraying quadcopter, the optimal hovering height is approximately 2 m. This can be further confirmed by comparing experimental results from field studies [20].

It is difficult for existing equipment to detect the distribution of the downwash flow planes experimentally. However, miniature UAV models can be used to develop airflow due to the consistent proportions. In addition, Laser Doppler Velocity (LDV) can also be used in experiments to detect airflow distribution [21].

3.2 Comparison of NACA 0015 and 4415 Aerodynamics

Based on the simulation stated that the curved airfoil NACA 4415 has better aerodynamic efficiency than the symmetrical airfoil NACA 0015. At the same time, better results and comparisons will provide proper research validation. NACA 4415 can produce a higher lift coefficient for the same area than NACA 0015. Between 10° < α 1 5° AOA, both NACA have good aerodynamic efficiency. Based on references, this is because the NACA 4415 profile, which has a curve, will provide greater pressure at the bottom of the profile and increase the airflow velocity at the top.

The flying speed of the drone used is 1 m/s, 2 m/s, 3 m/s, 4 m/s, and 5 m/s. This aerodynamic characteristic will affect the drone downwash effect that is produced when the drone is working so that the analysis at this point will affect the next point. Therefore, the results from a simulation of aerodynamic characteristics, which in this case are presented with CD and CL on drones with NACA 0015 and NACA 4415 propeller profiles (Table 3).

Table 3. Comparison of CD and CL at NACA 0015 and NACA 4415 based on CFD simulation

Velocity (m/s)	Propeller geometry			
	NACA 0015		NACA 4415	
	CD	CL	CD	CL
1	0.00170	0.178	0.00150	0.184
2	0.00172	0.189	0.00479	0.190
3	0.00324	0.197	0.00480	0.199
4	0.00472	0.221	0.007	0.231
5	0.00483	0.235	0.016	0.236

Based on the simulation data, by considering some of the same boundary conditions as the reference, it can be said that the simulation results follow the existing references where the aerodynamic characteristics of NACA 4415 are better than NACA 0015.

An upward trend occurs in both NACA profiles, directly proportional to the increased drone flight speed. The NACA 4415 profile has a higher value at each flight speed increase than NACA 0015. The downwash will be greatly affected by this event. The discussion regarding the downwash effect will be further explained in the next point.

3.3 Simulation Results of Downwash Flow Speed Distribution

The simulation result of downwash velocity distribution in flow visualization and data tables and graphs. Fig. 9 depicts the downwash flow velocity distribution on the drone during operation. The left image showcases a drone equipped with a propeller profile 0015, while the right image displays profile 4415. The visualization illustrates the distribution of the downwash flow for a predetermined speed parameter.

The visual comparison results are relatively insignificant. Notably, variations between the two propeller profiles are apparent. As the speed increases, the downwash flow distribution progressively moves away from the drone's position along the Y axis. This phenomenon occurs due to the relative airflow caused by the drone's velocity, consequently influencing the generated downwash flow (Fig. 10).

The simulation results indicate that the velocity distribution between the NACA 0015 profiles is greater than that of NACA 4415 at 10 points on the x and y axes. This difference is attributed to the symmetrical profile geometry of NACA 0015, allowing for higher airflow velocity through the propeller. Additionally, considering the aerodynamic characteristics of each profile mentioned earlier, NACA 0015 exhibits lower Cd and Cl values compared to NACA 4415, resulting in faster airflow through the NACA 0015 profile due to reduced drag (Fig. 11).

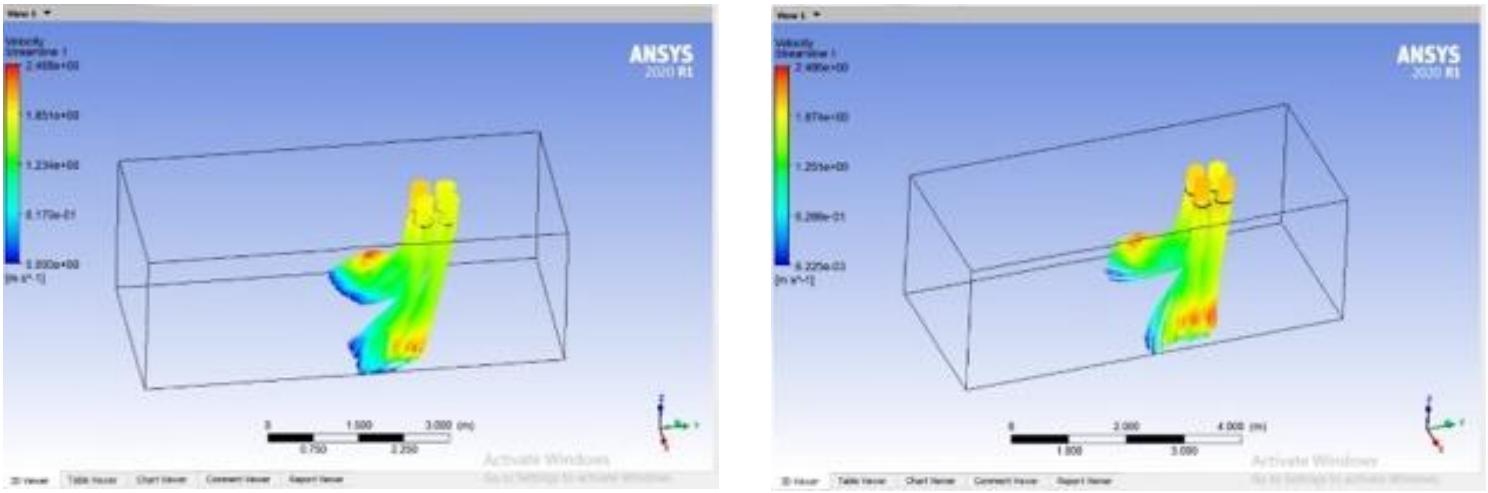

(a)

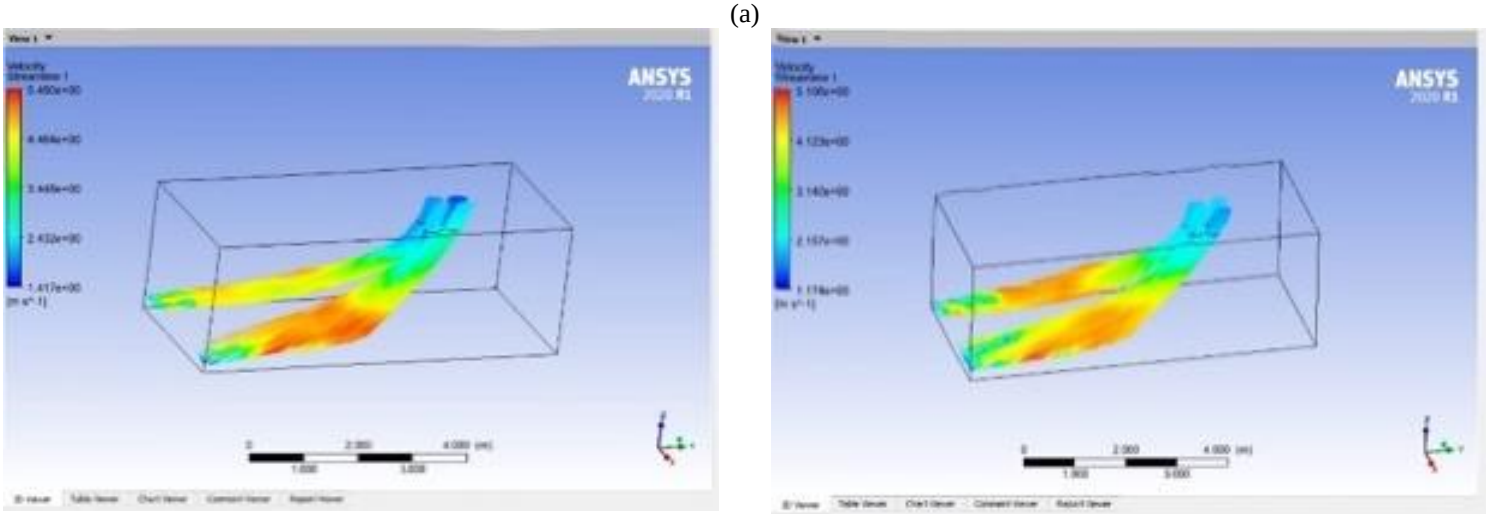

(b)

Fig. 9. Distribution of downwash flow velocity NACA 0015 and NACA 4415 (a) minimum flight speed 1 m/s, (b) maximum flight speed 5 m/s.

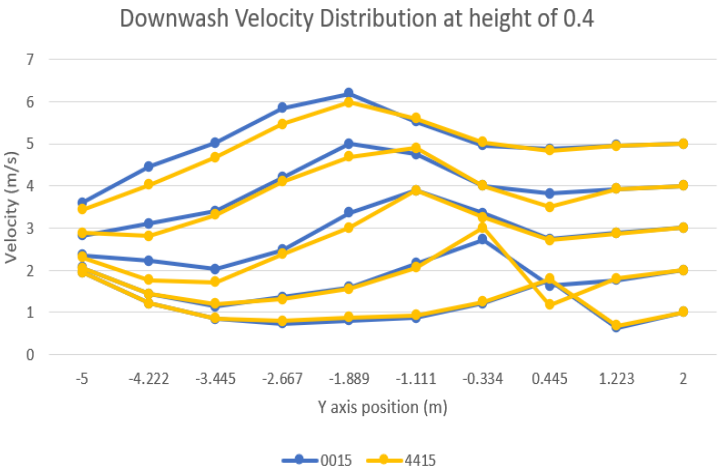

Fig. 10. Downwash velocity distribution on the Y axis at the height of 0.4 M NACA 0015 and NACA 4415.

Referring to the aerodynamic characteristics, the most significant distribution of the downwash speed is observed at the furthest points of the X and Y axes. Therefore, according to Table 4, the aerodynamic characteristics will experience an increase in the downwash speed value.

Fig. 12 is a visualization of the pressure distribution at a height of 0.4 m above ground level. The visualization shows the distribution area with different values. The visualization shows that the NACA 4415 profile has a relatively smaller maximum pressure distribution area compared to NACA 0015, meaning that the pressure distribution in NACA 4415 is more focused than NACA 0015.

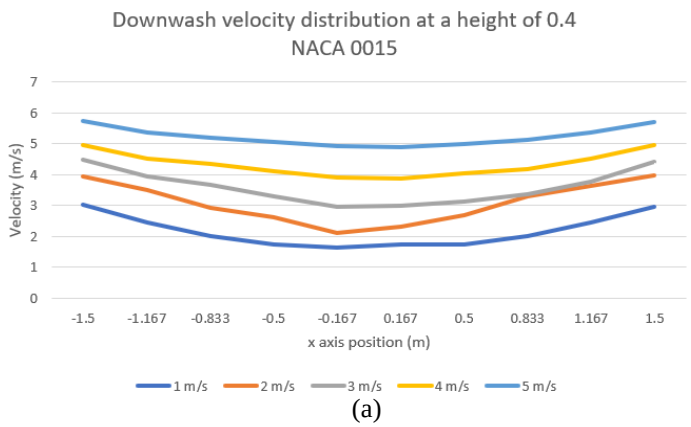

(a)

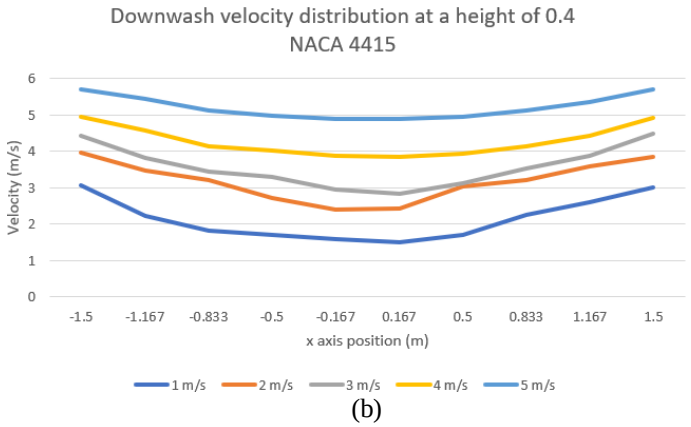

(b)

Fig. 11. Downwash velocity distribution on the X axis at a height of 0.4 M (a) NACA 0015 (b) NACA 4415.

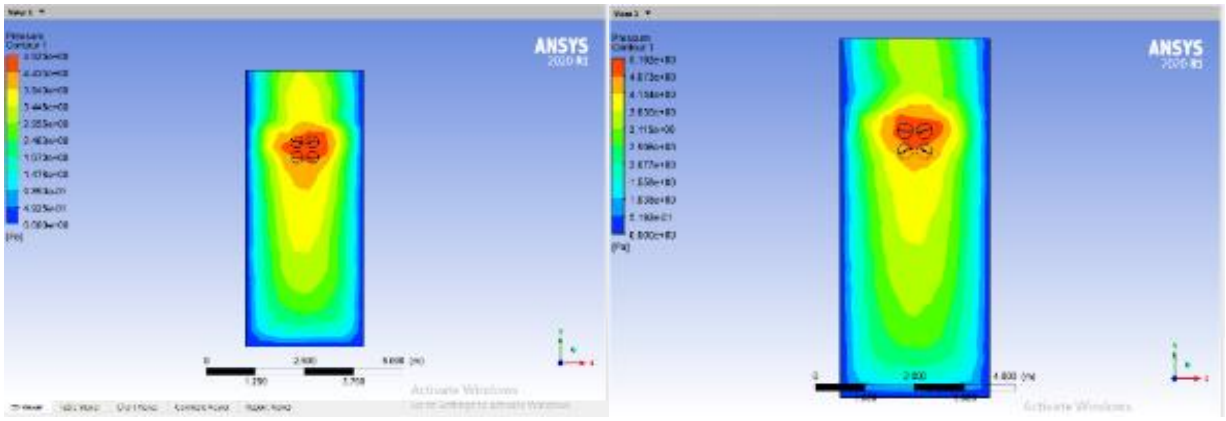

(a)

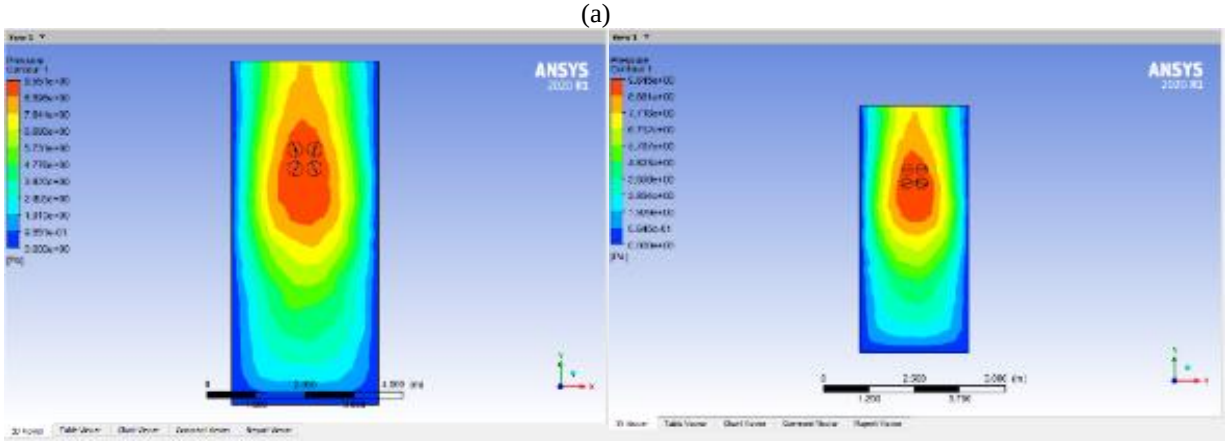

(b)

Fig. 12. NACA 0015 and NACA 4415 downwash flow pressure distribution (a) minimum flight speed 1 m/s, (b) maximum flying speed 5 m/s.

Fig. 13 and Fig. 14 are the results of data and graphs that will better explain the value of the downwash flow pressure distribution. The pressure distribution value is inversely proportional to the velocity distribution value. The maximum pressure distribution values are in the deepest of each X and Y axes.

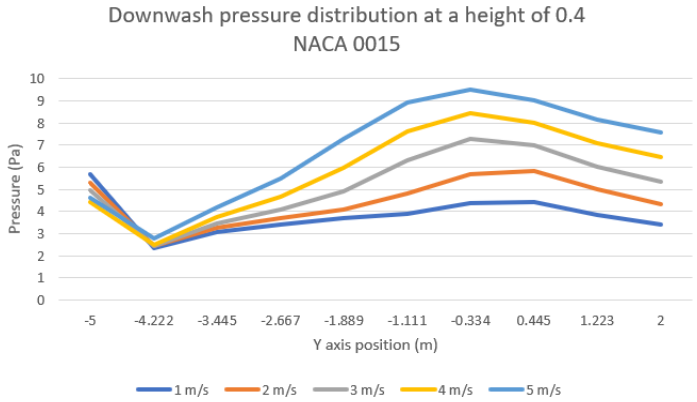

(a)

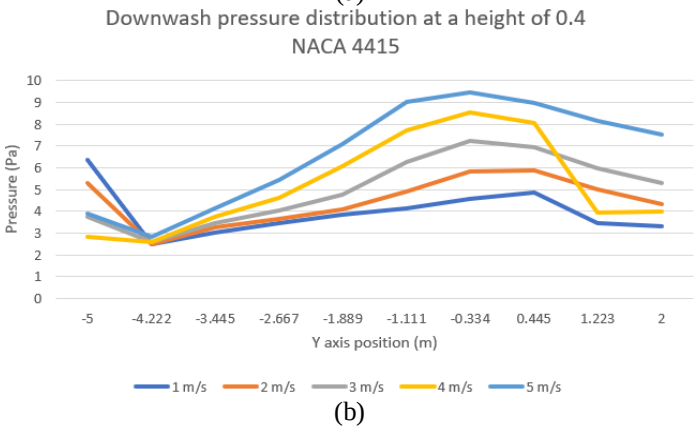

(b)

Fig. 13. Downwash pressure distribution on the y-axis at a height of 0.4 m (a) NACA 0015 (b) NACA 4415.

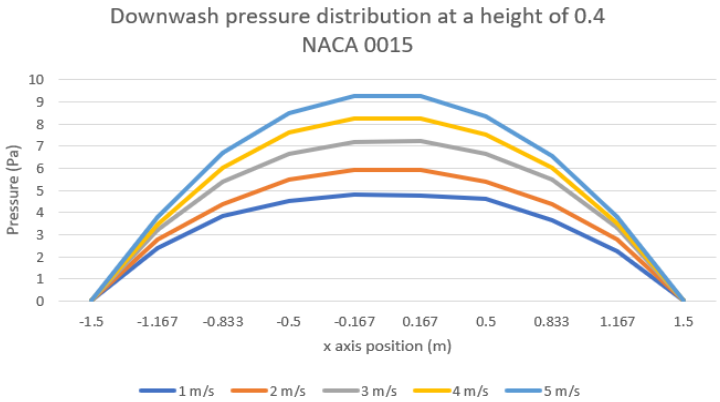

(a)

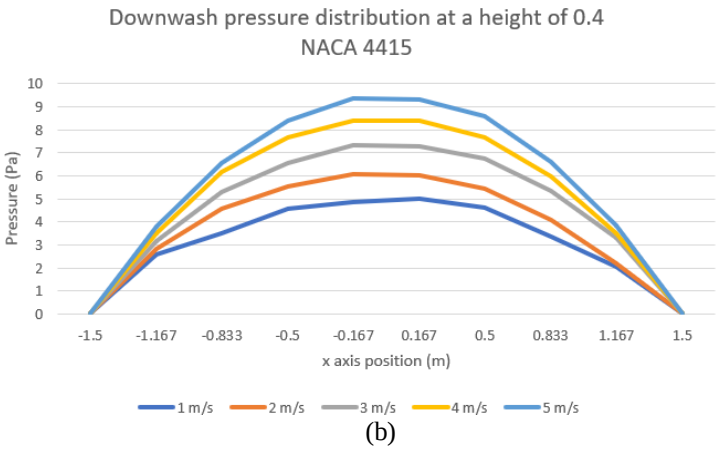

(b)

Fig. 14. Downwash velocity distribution on the x-axis at a height of 0.4 m (a) NACA 0015 (b) NACA 4415.

The increase in velocity factor affects the distribution of the downwash pressure distribution. With each rise in the area, the distribution of pressure distribution also increases the pressure value in both NACA profiles.

The aerodynamic characteristics affect not only the downwash speed but also the pressure. Therefore, it is intended that each increase in speed that increases Cd and Cl will also increase the pressure value. Besides that, it is related to the propeller geometry profile, namely NACA 0015 and 0045, which have Cd and Cl in NACA 4415 have a higher value so that the downwash pressure distribution value is also higher.

3.4 Range of Speed that can be Implemented

The maximum value of velocity and pressure distribution is obtained based on data from simulation results regarding downwash flow on rice plant protection sprinklers and comparisons on two NACA geometry profiles (Table 4).

Table 4. The maximum value of simulation downwash flow

Flight speed (m/s)	Maximum value of downwash distribution			
	NACA 0015		NACA 4415	
	Velocity (m/s)	Pressure (Pa)	Velocity (m/s)	Pressure (Pa)
1	3.04	5.679	3.056	4.989
2	3.968	5.911	3.094	6.061
3	4.478	7.297	4.476	7.315
4	4.964	8.442	4.952	8.556
5	5.968	9.843	5.714	9.472

Based on literature references concerning the wind resistance of rice plants [22], it has been determined that the maximum wind speed that rice plants can tolerate is 50 km/hour or approximately 13.8 m/s. However, the safe threshold for wind speed that rice plants can withstand is 20 km/hour or about 5.5 m/s.

The distribution of maximum downwash speed at NACA 0015 is more significant compared to that at NACA 4415. Conversely, the maximum downwash pressure distribution at NACA 0015 is smaller than that at NACA 4415. However, at a drone flying speed of 5 m/s, the maximum pressure at NACA 4415 is less than that at 0015. This indicates a decrease in performance pressure downwash at that particular speed.

Pressure downwash has a considerable impact on the spray droplet distribution area. Therefore, in order to achieve effective pesticide distribution, the droplet area should not exceed 2 m. Thus, the pressure and velocity should not surpass 2 m behind the drone's speed.

Based on these limitations, the recommended speed range for a plant protection sprinkler drone is approximately 1 m/s to 4 m/s. Previous research references regarding droplet distribution characteristics [23] suggest an optimal wind speed range of 2.3-2.8 m/s, thus supporting the recommendation of 2 m/s.

4 Conclusion

The downwash flow on rice plant protection drones was evaluated using the computational fluid dynamics method at various hovering heights. The speed and current distribution of the UAV were quite complex. The results indicated that as the hovering height increases, the minimum recent speed increased and then decreased. Additionally, an increase in hovering height led to a trade-off between factors such as spray range, deposition, and penetration uniformity, which could impact the spatial distribution of droplets and, subsequently, affect spraying effectiveness. Therefore, in practical operations, the quadcopter spraying plants maintained a hovering height of 2 m, a maximum velocity of 13.3 m/s, a minimum speed of 5,593 × 10-6 m/s, and a drone pressure of 0.03 Pa to achieve better downwash effects.

Increasing speed influenced the distribution of the downwash flow, causing it to spread further away from the drone in the opposite direction of the drone's speed. Moreover, as the aerodynamic properties improved, there was a direct increase in the downwash flow velocity distribution value in relation to the Cd and Cl values. Conversely, the downwash pressure distribution value exhibited an inverse relationship with the Cd and Cl concentrations. Consequently, the NACA 4415 exhibited greater Cd and Cl values, resulting in a lower downwash velocity distribution value compared to the NACA 0015. Conversely, the downwash pressure distribution value was higher at the same speed.

Based on the resistance of rice plants to wind speed and the characteristics of the downwash flow when the drone was working, the flight speed range that may be implemented on this plant protection sprinkler drone was 1-4 m/s, with an optimal recommendation of 2 m/s.

References

[1] J. D. Anderson, “Fundamentals of Aerodynamics (McGraw Hill Series in Aeronautical and Aerospace Engineering),” 2009.

[2] P. Velez, N. Certad, and E. Ruiz, “Trajectory Generation and Tracking Using the AR.Drone 2.0 Quadcopter UAV,” in Proceedings - 12th LARS Latin American Robotics Symposium and 3rd SBR Brazilian Robotics Symposium, LARS-SBR 2015 - Part of the Robotics Conferences 2015, Feb. 2016, pp. 73–78. DOI: 10.1109/LARS-SBR.2015.33.

[3] “Unmanned Aircraft Systems: Current and Potential Programs.” [Online]. Available: https://crsreports.congress.gov

[4] Y. bin Lan, S. de Chen, and B. K. Fritz, “Current status and future trends of precision agricultural aviation technologies,” International Journal of Agricultural and Biological Engineering, vol. 10, no. 3. Chinese Society of Agricultural Engineering, pp. 1–17, 2017. doi: 10.3965/j.ijabe.20171003.3088.

[5] A. Kirkaya, “Smart Farming- Precision Agriculture Technologies and Practices,” Journal of Scientific Perspectives, vol. 4, no. 2, pp. 123–136, Apr. 2020, DOI: 10.26900/jsp.4.010.

[6] U. R. Mogili and B. B. V. L. Deepak, “Review on Application of Drone Systems in Precision Agriculture,” in Procedia Computer Science, 2018, vol. 133, pp. 502–509. doi: 10.1016/j.procs.2018.07.063.

[7] H. Zhang et al., “Numerical analysis of downwash flow field from quad-rotor unmanned aerial vehicles,” International Journal of Precision Agricultural Aviation, vol. 1, no. 1, pp. 1–7, 2018, DOI: 10.33440/j.ijpaa.20200304.138.

[8] Y. Zheng et al., “The computational fluid dynamic modeling of the downwash flow field for a six-rotor UAV,” Front Agric Sci Eng, vol. 5, no. 2, pp. 159–167, May 2018, DOI: 10.15302/J-FASE-2018216.

[9] G. Vasconcelos, R. Sanches Miani, V. Guizilini, J. R. Souza, R. S. Miani, and V. C. Guizilini, “Evaluation of DoS attacks on commercial Wi-Fi-based UAVs,” 2019. [Online]. Available: https://github.com/jrsouza/alert_system.git

[10] S. Yang, Y. Zheng, and X. Liu, “Research status and trends of downwash airflow of spray UAVs in agriculture,” International Journal of Precision Agricultural Aviation, vol. 2, no. 1, pp. 1–8, 2019, DOI: 10.33440/j.ijpaa.20190201.0023.

[11] P. Zhang, W. Zhang, H. Sun, H. Fu, and J. Liu, “Effect Of The Downwash Flow Field Of A Single-Rotor Uav On Droplet Velocity In Sugarcane Plant Protection,” Engenharia Agricola, vol. 41, no. 2, pp. 235–244, 2021, DOI: 10.1590/1809-4430-ENG.AGRIC.V41N2P235-244/2021.

[12] N. Aneka, O. Tatale, S. Phatak, and S. Sarkale, “Quadcopter: Design, Construction, and Testing,” International Journal for Research in Engineering Application & Management, DOI: 10.18231/2454-9150.2018.1386.

[13] A. Bacchini and E. Cestino, “Electric VTOL configurations comparison,” Aerospace, vol. 6, no. 3, Mar. 2019, DOI: 10.3390/aerospace6030026.

[14] S. Krishnaraj, R. Senthil Kumar, A. Gokula Krishnan, G. Ganeshkumar, M. Mohan, and M. Nirmal, "Aerodynamic Analysis of Hybrid Drone," IOP Conf Ser Mater Sci Eng, vol. 1012, no. 1, p. 012023, Jan. 2021, DOI: 10.1088/1757-899x/1012/1/012023.
[15] R. Islam Rubel, M. Rokunuzzaman, R. R. I, U. M. K, and I. M. Z, "Comparison of aerodynamics characteristics of NACA 0015 & NACA 4415 aerofoil blade," Article in International Journal of Research-GRANTHAALAYAH, vol. 5, no. 11, p. 187, 2017, doi: 10.5281/zenodo.1095406.
[16] A. Mehrabi and A. R. Davari, "Outwash flow measurement around the subscale tandem rotor in ground effect," Engineering Science and Technology, an International Journal, vol. 23, no. 6, pp. 1374–1384, Dec. 2020, DOI: 10.1016/j.jestch.2020.08.016.
[17] R. Felismina, M. Silva, A. Mateus, and C. Malça, "Study on the aerodynamic behavior of a UAV with an applied seeder for agricultural practices," in AIP Conference Proceedings, Jun. 2017, vol. 1836. DOI: 10.1063/1.4981989.
[18] A. Tan Feng, L. Qi, M. Liu Chang-liang, and M. Jin Bing-kun, "Measurement Of Downwash Velocity Generated By Rotors Of Agriculture Drones / 植保无人机旋翼下洗气流速度的测量," 2018.
[19] E. Santosa and Y. Koesmaryono, "Morphological Mechanism and Physiology of Paddy Plants in Falling Conditions and Adaptation Strategies Watermelon breeding View project Elephant foot yam project View project Dulbari Dulbari Politeknik Negeri Lampung, Bandar Lampung, Indonesia," 2018. [Online]. Available: https://www.researchgate.net/publication/340004058
[20] S. Guo, J. Li, W. Yao, Y. Zhan, Y. Li, and Y. Shi, "Distribution characteristics on droplet deposition of wind field vortex formed by multi-rotor UAV," PLoS One, vol. 14, no. 7, Jun. 2019, DOI: 10.1371/journal.pone.0220024.
[21] Y. J. Zheng et al., "A novel detection method of spray droplet distribution based on LIDARs," International Journal of Agricultural and Biological Engineering, vol. 10, no. 4, pp. 54–65, 2017, DOI: 10.25165/j.ijabe.20171004.3118.